## Highlights

- Elemental chronologies of Ba and Sr were constructed for statoliths of *Doryteuthis gahi* using LA-ICP MS.
- Temporally distinct spawning cohorts had unique elemental chronologies.
- Elemental chronologies displayed significant variation throughout ontogeny.
- Cohort-specific chronologies were most dissimilar during 80-160 d post-hatching.
- Sr:Ca and Ba:Ca ratios were both negatively correlated with near-bottom water temperature.

# Using statolith elemental signatures to confirm ontogenetic migrations of the squid *Doryteuthis gahi* around the Falkland Islands (Southwest Atlantic)

Jessica B. Jones [a, b,*], Alexander I. Arkhipkin [a, b], Andrew L. Marriott [e], Graham J. Pierce [a, c, d]

[a] Oceanlab, University of Aberdeen, Main Street, Newburgh, Ellon, Aberdeenshire, AB41 6AA, UK

[b] Falkland Islands Fisheries Department, Stanley, FIQQ 1ZZ, Falkland Islands

[c] CESAM and Departamento de Biologia, Universidade de Aveiro, Av. Padre Fernão de Oliveira, 3810-193, Aveiro, Portugal

[d] Instituto de Investigacións Mariñas (CSIC), Eduardo Cabello 6, 36208, Vigo, Spain

[e] Inorganic Geochemistry, Centre for Environmental Geochemistry, British Geological Survey, UK

[*] Corresponding Author: JJones@fisheries.gov.fk

## Abstract

The Patagonian long-finned squid *Doryteuthis gahi* is an abundant commercial species within Falkland Island waters. The population consists of two temporally distinct spawning cohorts, inferred to have markedly different patterns of migration and timings of ontogenetic events. Ontogenetic migrations of each cohort were confirmed by analysis of the chemical composition of statoliths collected from both cohorts in two consecutive years. Trace element concentrations were quantified using laser ablation inductively coupled plasma mass spectrometry (LA ICP-MS), to determine temporal and cohort-specific variation. Individual ablation craters, ablated in a transect from the nucleus to the rostrum edge, were aged to produce high-resolution elemental chronologies. Generalised additive mixed models (GAMM) indicated that cohort and life history stage had a significant effect on Sr:Ca and Ba:Ca ratios.

Sr:Ca and Ba:Ca ratios were both negatively correlated with near-bottom water temperature, with Ba:Ca also potentially correlated to depth. Statolith elemental fingerprints have useful applications as natural tags, discriminating between spawning cohorts.

**Keywords**

*Doryteuthis gahi*, Laser Ablation ICP-MS, Trace Elements, Statolith, Migrations, Cephalopods

## 1 Introduction

Cephalopods have become an increasingly important fisheries resource over the last few decades, as evidenced by the rapid increase in global landings (Doubleday et al., 2016; Arkhipkin et al., 2015; Pierce and Portela, 2014; Hunsicker et al., 2010). They have an unusual life history characterised by; short lifespan, complex population structure and for many species extensive ontogenetic migrations. Understanding the degree of migration, connectivity and structure of a population is fundamental to the design of effective conservation and management strategies (Gillanders, 2005). Traditional techniques such as tagging allow for insights into an individual's movement and behaviour throughout ontogeny (Gilly et al., 2006; Thorrold et al., 2002). However, these techniques are difficult to implement on small species such as coastal loliginid squid, which are too fragile for an external tag and are lacking a suitable attachment site that does not inhibit their behaviour (Arkhipkin, 2005). An alternative method that requires no prior handling is the analysis of natural tags in the calcified structures of marine organisms. This method has been shown to have applications in determining population structure (Arbuckle and Wormuth, 2014), migration patterns ( Ikeda et al., 2003), assigning natal origin (Pecl et al., 2011) and as a proxy for environmental parameters (Beck et al., 1992). Analysis of elemental signatures has been applied to a wide range of taxa such as; scleractinian corals (Beck et al., 1992), teleost fish (Campana, 1999), gastropods (Zacherl et al., 2003), medusae (Mooney and Kingsford, 2012), bivalves (Gillikin et al., 2008) and cephalopods (Arbuckle and Wormuth, 2014; Warner et al., 2009).

Statoliths are paired calcareous concretions found within the statocysts, responsible for the detection of linear and angular acceleration in cephalopods (Arkhipkin and Bizikov, 2000; Clarke, 1978). Analogous to fish otoliths, these hard structures grow continually throughout life and are formed by the deposition of calcium carbonate crystals, primarily in aragonite form, within a protein matrix (Radtke, 1983). Throughout the accretion process, trace elements are incorporated into this matrix (Arkhipkin, 2005; Bettencourt and Guerra, 2000). Uptake of these elements into the statolith microstructure is considered to reflect the ambient environmental conditions at the time of incorporation. For example, Sr:Ca ratios have been suggested to have a negative relationship with temperature in many biogenic calcified structures in a wide range of taxa (Campana, 1999; Beck et al., 1992). Statoliths are appropriate for use as a natural tag on account of their metabolic inertness after deposition and the incorporation of continuous growth increments, which give a temporal scale for analysis (Wang et al., 2012).

The Patagonian long-finned squid *Doryteuthis gahi* (D'Orbigny, 1835) is a cold water loliginid most abundant in Falkland Island waters, where it is subject to an important and economically valuable commercial fishery. It is a small species, typically attaining an adult size of 13-17 cm mantle length (Arkhipkin et al., 2013). As well as being a key fisheries resource, *D. gahi* is involved in the transfer of organic and inorganic material across various parts of the shelf ecosystem and has an important role both as predator and prey (Arkhipkin, 2013). It is an important food source for marine mammals (Arkhipkin, 2013), commercially important finfish (Laptikhovsky et al., 2010) and seabirds (Piatkowski et al., 2001).

These squid undergo horizontal ontogenetic migrations from shallow inshore spawning and nursery grounds to feeding aggregations on the shelf edge and continental slope, where they are targeted by the fishery (Arkhipkin et al., 2004a; Hatfield et al., 1990). The fishery operates within two seasons corresponding to two temporally distinct cohorts (Patterson, 1988), the autumn spawning cohort (ASC) and spring spawning cohort (SSC), both of which have an annual life cycle. The duration of embryogenesis, extent of offshore migration and time of spawning differ between cohorts (Arkhipkin et al., 2013).

97 An initial study which determined the elemental composition of *D.gahi* statoliths using solution-based
98 inductively coupled plasma mass spectrometry (ICP-MS) found significantly different elemental
99 signatures between cohorts and geographic regions (Arkhipkin et al., 2004a). As the study dissolved
100 the entire statolith and quantified its elemental composition, it was unable to determine how the
101 elemental signal changed throughout ontogeny. Alternative analytical techniques such as laser probe
102 or laser ablation analysis are able to target specific regions of the statolith microstructure to gather stage-
103 specific information on life history and migration patterns.

104 A good understanding of migration patterns is of particular importance in short-lived species such as
105 *D. gahi*, which show a strong inter-annual variability and are more sensitive to factors such as increased
106 fishing pressure and environmental change (Doubleday et al., 2016). Therefore, the aims of this study
107 were to generate temporally resolved elemental chronologies for each individual by quantifying trace
108 elements in statoliths, to compare the elemental chronologies generated for each spawning cohort and
109 to explore possible relationships between environmental factors and the element:Ca ratio at the
110 corresponding time of incorporation.

111

112 **2 Materials and methods**

113 *2.1 Statolith Collection and Preparation*

114 Squid were collected and frozen by scientific observers on board commercial trawling vessels within
115 the Falkland Islands Interim Conservation and Management Zone (FICZ). Data collection took place
116 during both fishing seasons (Season 1: March-May, Season 2: July-October) of both 2014 and 2015
117 within the designated fishing zone, the "Loligo box" and to the west of the Falkland Islands (Fig. 1).
118 Mature individuals of both sexes were selected to ensure that each individual had a long elemental
119 chronology representing as many life history stages as possible (Table 1).

120

**Figure 1: Sample locations within the Falkland Interim Management and Conservation Zone (FICZ). The Loligo box denotes the fishing area. Monthly oceanographic data were collected along the CTD transect (dotted line). The inset map indicates the position of the Falkland Islands in relation to mainland South America.**

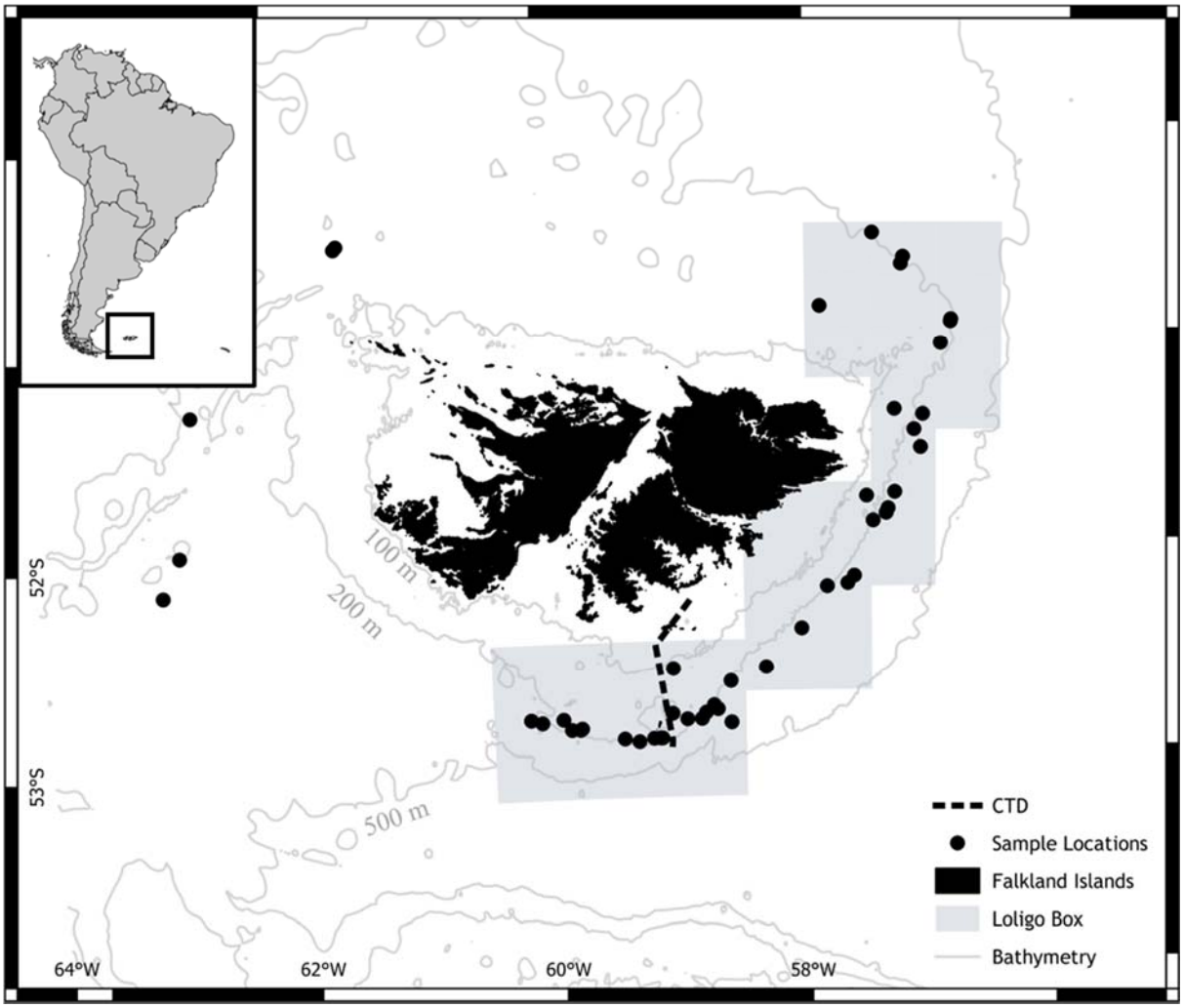


Squid samples were processed in the Falklands Island Fisheries Department laboratory. Samples were measured (dorsal mantle length ± 1 mm), weighed (total weight ± 1 g) and visually assessed for sex and maturity stage according to Lipinski (1979). Statoliths were dissected from the cephalic cartilage and stored in 96% ethanol. One statolith per specimen was mounted for elemental and age analysis concave side up, then ground and polished on one side to expose the nucleus (Arkhipkin and Shcherbich, 2012).

**Table 1: Summary of samples collected. N = number of samples collected.**

| Collection Year | Cohort | Mean Collection Depth (m) | Sex | N | Mantle Length (cm) | Age range (days) | Mean age (days) |
|---|---|---|---|---|---|---|---|
| 2014 | ASC | 185 | M | 23 | 9.0-34.5 | 181-322 | 241.8 |
| | | | F | 11 | 9.0-18.0 | 185-274 | 223.7 |
| | SSC | 230 | M | 49 | 7.0-38.0 | 152-312 | 252.7 |
| | | | F | 11 | 8.5-16.5 | 173-237 | 205.2 |
| 2015 | ASC | 178 | M | 34 | 10.0-33.0 | 169-289 | 226.9 |
| | | | F | 21 | 10.5-20.0 | 165-258 | 218.7 |
| | SSC | 230 | M | 24 | 10.0-31.5 | 171-288 | 227.6 |
| | | | F | 12 | 10.0-21.5 | 163-248 | 206.1 |

*2.2 Trace Element Analysis*

Statoliths were analysed using laser ablation inductively coupled plasma mass spectrometry (LA ICP-MS) at the British Geological Survey, Nottingham. Ground statoliths (n = 271) were remounted using Crystalbond 555 in batches of 12, with contaminants removed from the ground surfaces using a solution of 1% $HNO_3$/ 0.5% HCL prior to analysis. Elemental concentrations were obtained using a 193 nm Class 4 Nd: YAG solid state excimer lamp-pumped laser ablation system (New Wave Research, USA) coupled with an *in situ* Agilent 7500c ICP-MS. The following trace elements were quantified at each ablation spot; $^{23}Na$, $^{88}Sr$, $^{24}Mg$, $^{11}B$, $^{7}Li$, $^{138}Ba$, $^{27}Al$, $^{55}Mn$, $^{56}Fe$, $^{66}Zn$, $^{63}Cu$, $^{114}Cd$ and $^{208}Pb$, with $^{42}Ca$ used as an internal standard to account for variation in ablation yield.

Equally incremented ablations (35 µm ⌀, spacing 70 µm) were made along the axis of growth from the nucleus to the marginal edge of the rostrum (Fig. 2). The number of ablation sites ranged from 12 to 20 per statolith depending on statolith total length, which has been shown to have a linear relationship with mantle length (Hatfield, 1991). Ablation parameters were as follows; a pulse rate of 10 Hz with an average irradiance of 0.67 GW/cm$^2$, an average fluence of 3.33 GW/cm$^2$ and a dwell time on each ablation spot of 30 s. Ablated material was transferred from the laser ablation cell to the ICP-MS in a flow of helium (0.8 l min$^{-1}$) which was then combined with a stream of argon carrier gas (0.9 l min$^{-1}$).

Due to a lack of appropriate matrix matched calibration standards, the glass reference materials NIST-610 and NIST-612 (National Institute of Standards and Technology, USA) were used for external

153 calibration. NIST-610 was ablated at the start and end of each slide, and after every fourth sample to
154 calibrate elemental concentrations and assess changes in instrumental sensitivity. NIST-612 was
155 measured at the start of each slide and treated as an unknown sample to assess measurement accuracy
156 (Limbeck et al., 2015). Periods of gas blank collected for 40 s prior to each ablation were defined as
157 background, the average of which was subtracted from subsequent samples. Raw counts (cps) of each
158 element were processed using Igor Pro 6. 34 (WaveMetrics) with the extension package Iolite v. 2.5.

159 *2.3 Age Estimation*

160 Ablated statoliths were flipped and ground on the other side, overturned again to better visualise
161 ablation craters, embedded in mounting medium (Canada Balsam ™) and covered with a cover glass
162 for observation. Statoliths were read under the transmitted light of an Olympus BX51 compound
163 microscope at x400 magnification, with a phase-contrast Nomarski effect used to improve readability
164 (Arkhipkin and Shcherbich, 2012).

165 Statoliths were first read in the lateral dome from the natal ring to the first prominent check. This check
166 was followed into the rostrum and read in the rostrum to the tip. As the one ring=one day hypothesis
167 has been validated in other loliginid species (e.g. *Loligo plei* [Jackson and Forsythe, 2002], *Loligo*
168 *vulgaris reynaudii* [Lipinski et al., 1998], *Sepioteuthis lessoniana* [Jackson et al., 1993]), total
169 increment number was assumed to represent post-embryonic age in days. To minimise counting errors,
170 total number of growth increments for each specimen was taken as the mean of at least two counts. If
171 the difference between these counts exceeded 10% a third count was made. If the difference between
172 the second and third readings still exceeded 10% the statolith was rejected from further age analysis. A
173 sub-sample of 10 statoliths was counted by a second reader to further minimise error (First reader J.
174 Jones, second reader A. Arkhipkin). A total of 272 statoliths was prepared, of which 185 (68%) were
175 successfully ablated and read. Statoliths were discarded throughout the process either because 1.)
176 Ablation craters were too shallow to be visualised under the microscope for ageing 2.) The statolith was
177 over ground or 3.) Initial data exploration suggested contamination, indicated by the combined presence

178 of Zn, Cu and Fe. This has been indicated to be a common issue during elemental analysis of statoliths
179 (Arbuckle and Wormuth 2014).

180 Hatch date was determined by back-calculation of total number of increments (=age in days) from the
181 date of capture. Based on hatch date, each squid was assigned to a spawning cohort; those with hatch
182 dates in July – October were assigned to the ASC and those with hatch dates from November – May
183 were assigned to the SSC (Arkhipkin et al., 2004a). Each individual ablation spot was aged to produce
184 time-delimited elemental signatures. Visual inspection indicated that each ablation spot represents
185 approximately one week during an individual's life. The central growth ring of each ablation spot was
186 considered to be the ablation spot age (days post hatching - Fig. 2).

187 **Figure 2: Image of ground statolith. Region delimited by the white line contains 6 growth increments. Lines between**
188 **growth increments are optical effects. Circles indicate regions where material has been ablated. Inset image shows a**
189 **statolith with 12 ablation spots from the nucleus to the rostrum edge.**
190

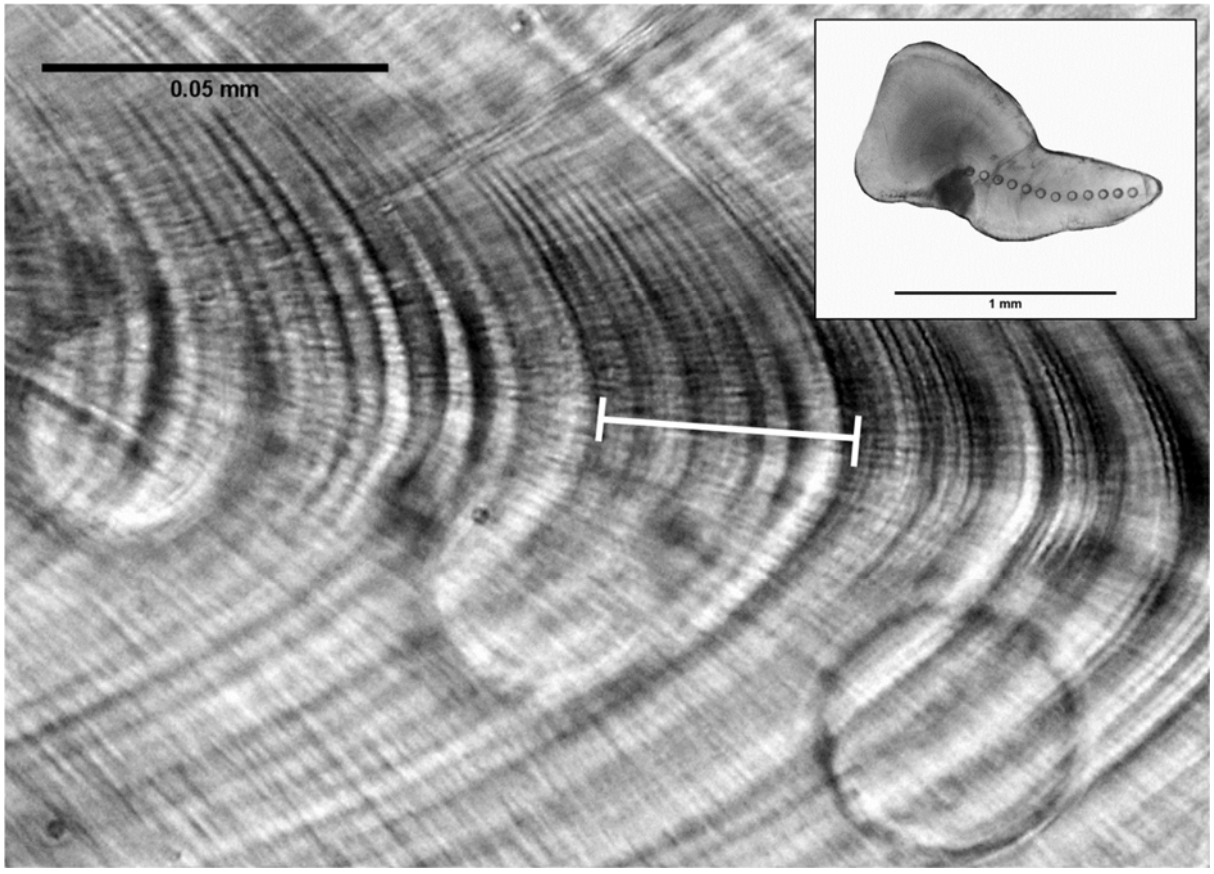


191

192 *2.4 Oceanographic Data Collection*

193 Monthly oceanographic data have been routinely collected by the Falkland Islands Fisheries
194 Department on board the Falkland Islands fisheries patrol vessel (Fig. 1). These data were collected
195 along a transect located in the southern part of the "Loligo box" using a SeaBird Electronics SBE 25
196 CTD (Sea-Bird Electronics Inc. Bellevue, WA, USA). Transects were carried out approximately mid-
197 month subject to vessel availability and weather conditions. The CTD was lowered to the seabed and
198 retrieved at a rate of 1 $ms^{-1}$. Temperature ($^{o}C$) was measured directly and salinity (PSU) was derived
199 from conductivity ($S\ m^{-1}$) using Seasoft v. 4.326 software (Sea-Bird Electronics Inc.). Transect stations
200 (with depths of 55 m, 60 m, 100 m, 200 m and 300 m) covered the reported species depth range
201 (Arkhipkin et al., 2013). Near-bottom temperature and salinity profiles were interpolated for each
202 transect using data collected from May 2013 to December 2015.

203 *2.5 Statistical Analysis*

204 Values for limit of detection (LOD) were calculated as 3 standard deviations of the background signal.
205 Mean values for LOD (ppm) were; $^{7}$Li, 0.183; $^{11}$B, 2.381; $^{23}$Na, 22.807; $^{24}$Mg, 0.581; $^{27}$Al, 1.298; $^{55}$Mn,
206 1.207; $^{56}$Fe, 1.663; $^{63}$Cu, 0.833; $^{66}$Zn, 0.269; Sr, 1.373; $^{114}$Cd, 0.167 $^{138}$Ba, 0.018; and $^{208}$Pb, 0.022.
207 Elements Pb, Cu, Zn, Fe, Al, Cd and B were consistently below the theoretical LOD and were
208 subsequently removed from further analysis. Each element was standardised to calcium to produce
209 element/Ca ratios and further analysed in R V.3.3.0 (R Core Team, 2016). For the purposes of this
210 study, only Sr/Ca and Ba/Ca ratios were investigated, as these are often cited to have a relationship with
211 environmental parameters.

212 Data exploration was undertaken following procedures described in Zuur et al., (2009). Extreme
213 outliers observed in Cleveland dotplots were removed prior to analysis. For visual presentation,
214 element:Ca ratios for individual ablation spots were pooled by the number of weeks post-hatching,
215 separately for both assigned cohorts. Mean concentrations for each week were plotted with a 3-point
216 moving average applied to improve visualisation. However, for statistical modelling raw post-hatching
217 age in days were used.

The data set consisted of multiple time observations for each squid (or statolith). We therefore applied two generalised additive mixed models (GAMM), one using Sr:Ca ratios and the other using Ba:Ca ratios as the response variable, with the random effect statolith number (a unique identifier for each individual) nested within cohort as a way to model dependency (Zuur and Ieno, 2016). Statistical modelling was performed in the R package "mgcv" (Wood, 2006).

A Gaussian GAMM (identity link) was used for Sr:Ca (Equation 1) and Ba:Ca (Equation 2) to determine whether element:Ca ratios could be linked with cohort assignment and ontogenetic time.

Fixed covariates available were sex (categorical with two levels), year (of collection; categorical with two levels) and cohort (categorical with two levels). The addition of an interaction term between year and cohort were investigated. A categorical variable of cohortyear (with 4 levels: ASC-2014, SSC-2014, ASC-2015 and SSC-2015) was also investigated and compared to model performance with cohort and year included as separate factors. The variable day (within the year, a categorical variable ranging from 1-365) had a smoother fitted using cyclic cubic regression splines, penalised cubic regression splines whose ends meet up. The remaining variable, age (number of days post-hatching) is continuous and a smoother was fitted using thin plate regression splines (Wood, 2003). To incorporate the dependency among observations of the same statolith, we treated Statolith.no as a random variable. The random effect of location was also explored, using station as a proxy to capture the spatial component (each station was a unique trawl identifier, with each trawl having a different spatial location).

Equation 1:

$$g\left(E\left(Sr_{ij}\right)\right) = Statolith.no_i + f_{ij}(Age \times Cohort) + Cohort \times Year + \varepsilon_i$$
$$\varepsilon_i \sim N(0, \sigma^2)$$

Equation 2:

$$g(E\left(Ba_{ij}\right)) = Statolith.no_i + f_{ij}(Age\ x\ Cohort) + Cohort + \varepsilon_i$$
$$\varepsilon_i \sim N(0, \sigma^2)$$

240 Where element$_{ij}$ is the $j^{th}$ observation in Statolith.no $i$, and $\varepsilon_i$ is the random intercept, which is assumed
241 to be normally distributed with mean 0 and variance $\sigma^2$.

242

243 Examination of residuals suggested a transformation was necessary to avoid violating the assumptions
244 of normality and to reduce heterogeneity. A box-cox transformation was applied (Box and Cox, 1964)
245 which improved the residual fit, defined as:

246 $$y_i{}^{\lambda} = \begin{cases} \dfrac{y_i{}^{\lambda} - 1}{\lambda_i}, & \lambda \neq 0 \\ \ln y, & \lambda = 0 \end{cases}$$

247 Optimal GAMs were selected via backwards selection on the basis of the lowest value of Akaike
248 Information Criterion (AIC), providing that there were no serious patterns in residuals and all remaining
249 explanatory variables had a significant effect. The mixed model random components were then added
250 to the optimised GAM.

251

252 **3 Results and discussion**

253 *3.1 Temporally resolved elemental ratios*

254 Growth ring analysis indicated an age range of 152 – 322 d and a mean age of 233 d (Table 1).
255 Elemental concentrations of *D. gahi* statoliths, expressed as ratios:Ca are displayed in Table 2 for
256 elements which concentrations were normally above the LOD. The mean values for each element:Ca
257 ratio were generally similar to those found in the previous solution-based ICP-MS study on *D. gahi*
258 (Arkhipkin et al., 2004a), which reported an approximate Sr:Ca ratio of 8 mmol.mol $^{-1}$ (this study μ =
259 9.46 mmol.mol $^{-1}$) and Ba:Ca ratios ranging from 3 to 8 μmol.mol $^{-1}$ (this study 4-16 μmol.mol $^{-1}$).
260 Mn:Ca ratios were also similar, ranging from 0.02-9.9 μmol.mol$^{-1}$ (1-3 μmol.mol$^{-1}$ in the previous
261 study). However, the ranges of values found in the present study are much broader for each element.
262 In particular, Mg (30 – 535 μmol.mol$^{-1}$) had a much broader range than the previous solution based

study (70 – 170 μmol.mol$^{-1}$). This is likely to be due to methodical differences. If element concentrations vary widely across an individual statolith, this would not be apparent in a study based on measurements for whole statoliths. It is also possible that measurement error is higher for the ablation method, however sampling procedures ensured that measurement error (due to instrumental drift and high sensitivity detecting contaminants) was minimized. The present study is consistent with the previous study (Arkhipkin et al., 2004a) in that elemental signatures of *D.*gahi varied significantly geographically and between spawning cohorts.

**Table 2: Summary of element:Ca ratios for *D.gahi* statoliths.**

| Element | Minimum | Maximum | Mean ± SD |
|---|---|---|---|
| Na:Ca (mmol.mol$^{-1}$) | 16.18 | 28.39 | 20.48 ± 1.47 |
| Sr:Ca (mmol.mol$^{-1}$) | 5.84 | 14.57 | 9.46 ± 1.24 |
| Mg:Ca (μmol.mol$^{-1}$) | 33.89 | 535.38 | 140.43 ± 76.23 |
| Li:Ca (μmol.mol$^{-1}$) | 0.58 | 280.47 | 33.13 ± 34.10 |
| Ba:Ca (μmol.mol$^{-1}$) | 4.52 | 16.54 | 7.73 ± 1.48 |
| Mn:Ca (μmol.mol$^{-1}$) | 0.02 | 9.89 | 2.61 ± 1.26 |

Typically, laser ablation studies using statoliths as sample material involve fewer than 40 individuals. This is the first study to conduct this type of analysis on a much larger scale, allowing for cohort-specific temporally resolved elemental fingerprints to be generated, as observed in Fig. 4B and 4D. For both Sr and Ba, element:Ca ratios exhibited considerable ontogenetic variation and the elemental fingerprints for each cohort are noticeably different. Cohort-specific elemental signatures affirmed the results of Arkhipkin et al., (2004a), with the inclusion of separate smoothers (for the Age effect) for the ASC and SSC significantly improving the model fit for both response variables, as shown by analysis of deviance (Sr model: $F = 6.65$, $p < 0.05$, Ba model: $F = 11.01$, $P < 0.05$). The chemical composition of statoliths from the ASC and SSC are most dissimilar during 80-160 days post-hatching (12-23 weeks) where a clear gap is seen between the 95% confidence intervals of the two cohorts (Fig. 3).

**Figure 3: Fitted curves based on model predictions for the concentration of A – Ba:Ca and B- Sr:Ca (on box-cox transformed scale) ratios in relation to post hatching age in days, with individual smoothing curves constructed for each cohort and 95% confidence intervals included.**

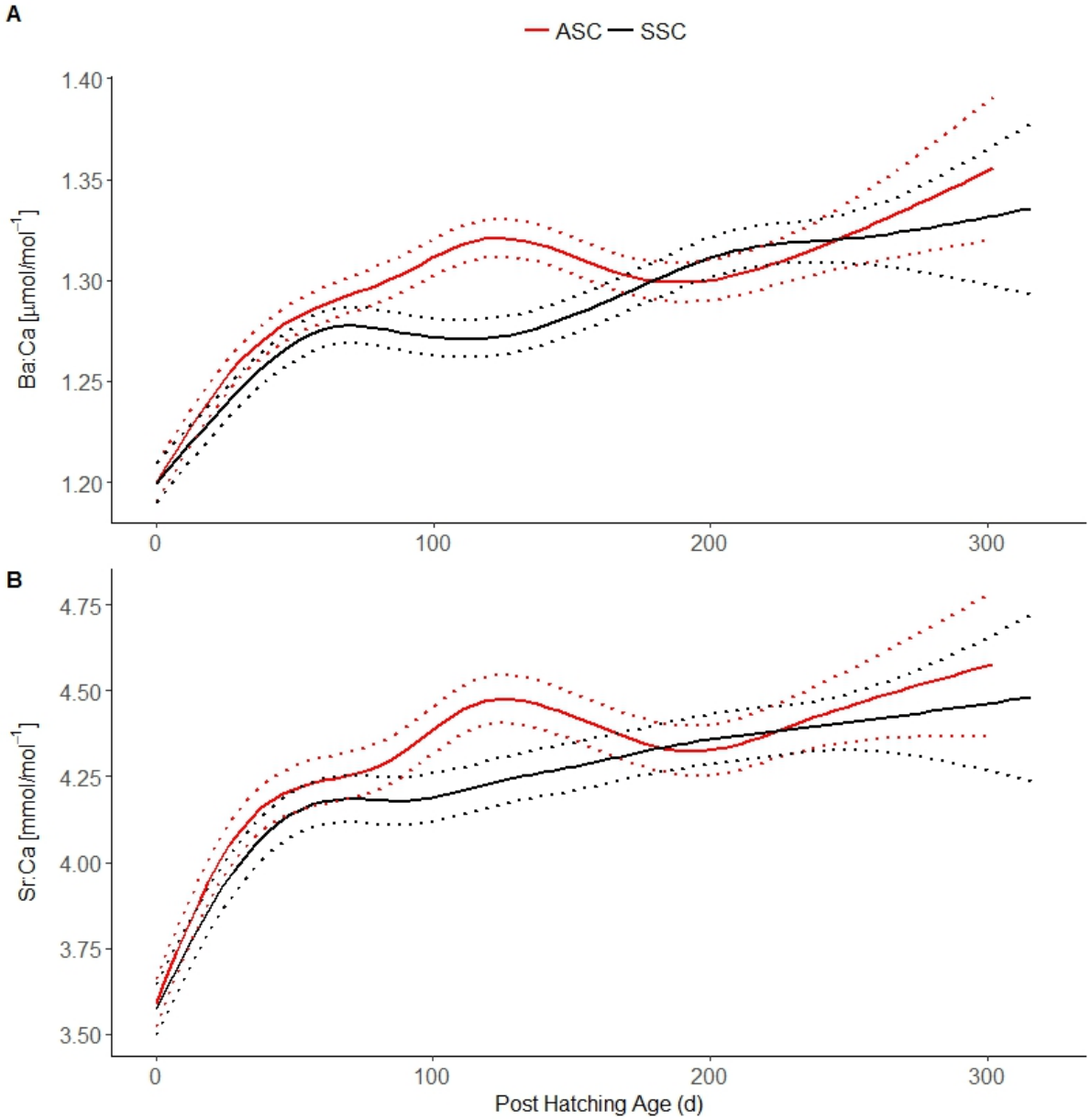


Modelling results are found in Table 3 and confirmed that time during ontogeny (squid age), and cohort assignment were significantly related to element:Ca concentration for both Sr ($R^2 = 0.37$) and Ba ($R^2 = 0.28$). Although year itself was not significant, the interaction between year and cohort was significant for strontium ($t = 2.01$, $p = 0.04$). Contrary to the solution-based study (Arkhipkin et al., 2004a), inclusion of a spatial component in the model did not improve fit, implying that no significant difference could be found in elemental signatures from different geographic locations.

**Table 3 Estimated regression parameters for two-way nested generalized additive mixed models (GAMM) for the response variables Sr:Ca and Ba:Ca, as presented in eqn (1) and eqn (2). t values and P values are included, as well as expected degrees of freedom (edf) for smooth terms. Significance, *** = p<0.0001, ** = p<0.01, * = p<0.05.**

| Response variable | Explanatory variable | edf | F value | P-Value |
|---|---|---|---|---|
| Sr:Ca | Cohort | - | -3.07 | < 0.05** |
| | Year | - | -0.63 | 0.52 |
| | Cohort:Year | - | 2.01 | < 0.05* |
| | Days:Cohort_ASC | 7.65 | 178.6 | < 0.05*** |
| | Days:Cohort_SSC | 7.35 | 156.5 | < 0.05*** |
| Ba:Ca | Sex | - | -2.99 | < 0.05** |
| | Days:Cohort_ASC | 6.69 | 121.4 | < 0.05*** |
| | Days:Cohort_SSC | 6.20 | 101.8 | < 0.05*** |

*3.2 Sr:Ca ratios*

Ontogenetic variation in mean Sr:Ca ratio for both cohorts (ASC and SSC) and consecutive years (2014 and 2015) is shown in Fig. 4B. In all four groups there is a spike in Sr concentration during the first 5 weeks of life, with each individual's Sr:Ca ratio increasing by approximately 1.5 mmol.mol $^{-1}$ during this early stage of ontogeny. Aside from this common pattern, the elemental signatures are markedly different for each cohort; The general trends for the ASC cohort is an increase in Sr:Ca concentration with a corresponding decrease during February - March. The SSC cohort is characterised by a progressive increase in Sr:Ca ratio over time. This is also observed in the fitted smoothing curves from the GAMM model in Fig. 3B. The smoothing curve applied to the SSC had lower expected degrees of freedom than the ASC indicating a less complex trend, closer to linear (Table 3).

**Figure 4: A –Seasonal changes in near-bottom temperatures at various depths on the Falkland Islands shelf overlaid with a scheme of the ontogenetic migrations of the ASC (grey) and SSC (black). Circles indicate periods of egg devlopment. B –Sr:Ca elemental fingerprints for the ASC (grey) and SSC (black) in 2014 (dashed line) and 2015 (line). C –Seasonal changes in near bottom salinity . D – Ba:Ca elemental fingerprings for the ASC (grey) and SSC (black) in 2014 (dashed line) and 2015 (line).**

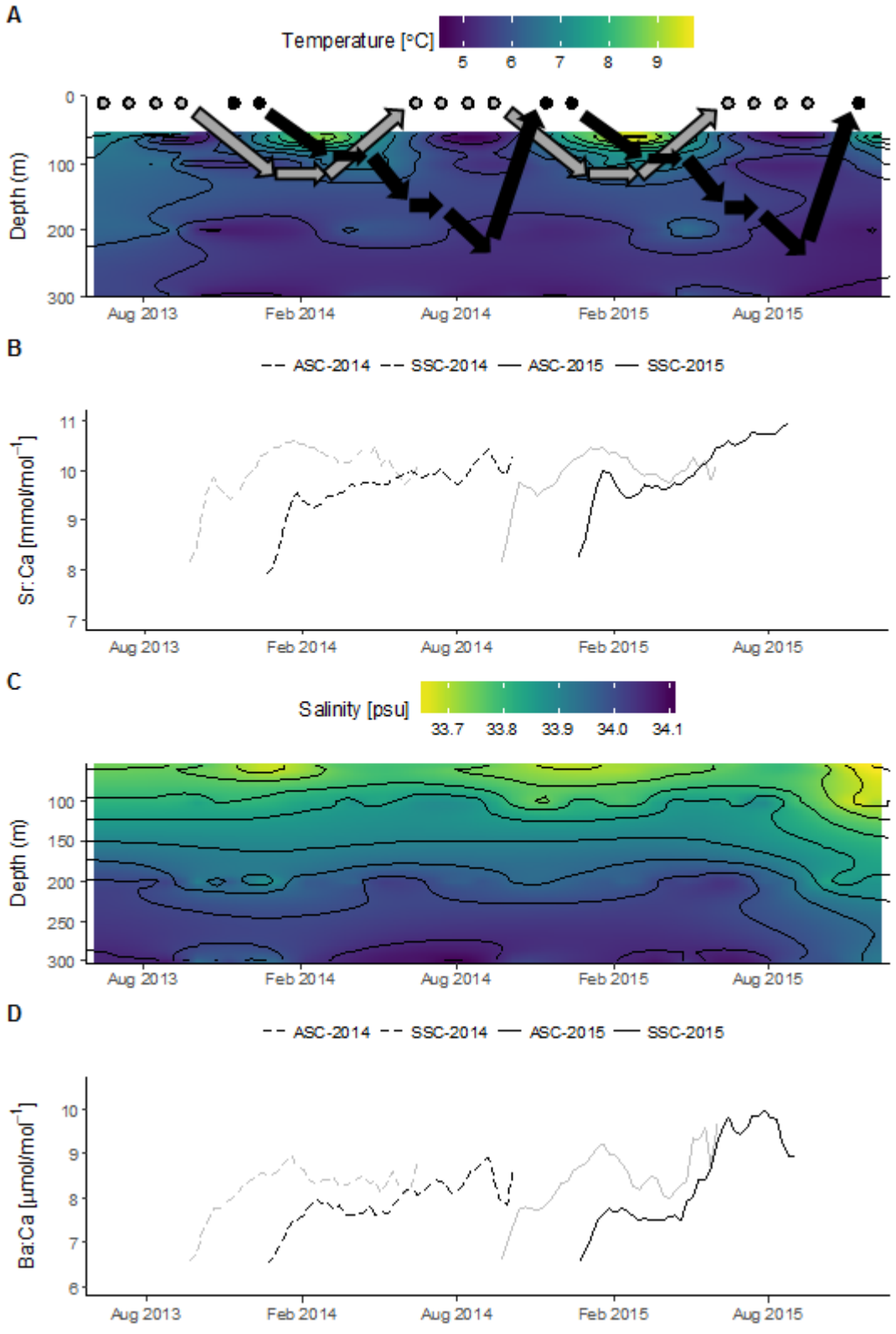


It is evident from the cohort-specific ontogenetic patterns that Sr:Ca ratios show high potential to discriminate between population components. An investigation into how elemental patterns (obtained from 5-6 ablation spots per statolith) vary between geographically separate groups of the Humboldt

squid *Dosidicus gigas* similarly found that Sr:Ca ratios were significantly different between population sub-groups (Arbuckle and Wormuth, 2014). Geographical variation in Sr:Ca ratios were also found when comparing two groups of the ommastrephid squid *Todarodes pacificus* in the Sea of Japan (Ikeda et al., 2003). Nevertheless, to date the only squid found to have cohort-specific differences in the Sr:Ca elemental signature has been *D.gahi*. The only other study comparing spawning cohorts, which analysed the multivariate elemental signatures of the ommastrephid squid *D. gigas*, found no significant differences between three cohorts (Liu et al., 2015). Unlike loliginids, ommastrephid squid undergo extensive diel-vertical migrations that are likely to mask the patterns arising from horizontal migration (Arkhipkin et al., 2004a).

The dynamics of incorporation of trace elements into calcified structures of organisms may be regulated by many different factors, both intrinsic and extrinsic in nature, for example; physiology, ontogenetic stage, reproduction, diet, stress level, temperature, salinity and water chemistry (Radtke and Shafer, 1992). In reality, the chemical composition of calcified tissues is most likely driven by a multiplicity of factors at any particular moment of a squid's life; however the primary factors driving the deposition are likely to be different for each trace element. Many experimental studies have shown a strong association between Sr:Ca ratios and temperature. An inverse relationship was first found in scleractinian corals (Beck et al., 1992; Smith et al., 1979) and was later found in a wide range of marine taxa. In cephalopods, field studies have inferred a negative relationship between Sr:Ca and temperature based on existing knowledge of the species life cycle (Liu et al., 2016; Liu et al., 2013; Zumholz et al., 2007b; Arkhipkin et al., 2004a). In the herring *Clupea harengus*, laboratory experiments indicated that the greatest temperature effect occurred at lower temperatures, with temperatures less than 5 $^{o}$C physiologically impairing their ability to discriminate against the incorporation of strontium into the otolith (Townsend et al., 1992). As *D.gahi* is the coldest water loliginid, inhabiting near-bottom waters with minimum temperatures of ~ 4.9 $^{o}$C, the temperature effect on strontium uptake may be pronounced for this species.

Water chemistry and diet are also thought to be drivers of Sr incorporation in calcified tissues. The dietary effect on Sr incorporation was found to be up to 10% in experimental studies on statoliths of the

cephalopod *Sepia officinalis* (Zumholz et al., 2006). For the damselfish *Acanthochromis polyacanthus*, effects of ontogenetic stage and diet interacted to drive the incorporation of Sr (Walther et al., 2010). In terms of water chemistry, dramatic drops in Sr:Ca values have been associated with ontogenetic movements from seawater, relatively rich in Sr to low-Sr freshwater environments (Radtke et al., 1988).

*D. gahi* inhabits near-bottom layers of the Patagonian shelf and undergoes extensive inshore-offshore ontogenetic migrations from shallow nursery grounds to deep offshore feeding grounds on the shelf edge (Arkhipkin et al., 2013). This species therefore experiences significant variation in a multitude of environmental factors during migration which may affect elemental uptake into the statolith microstructure. Although squid of both cohorts have an annual life cycle and occur on the same feeding grounds (Agnew et al., 1998; Patterson, 1988), differences in the timing of ontogenetic events such as spawning and hatching, and inter-annual fluctuations in temperature and salinity mean that they are subject to very different environmental conditions throughout their lifetime (Arkhipkin et al., 2013). Therefore, when comparing elemental profiles to environmental events, profiles for each cohort should be considered separately.

A schematic diagram of the life-cycle of each cohort is presented in Fig. 4A. Post-hatching juveniles and paralarvae of the ASC remain inshore in shallow nursery grounds, undertaking gradual offshore migration to feeding grounds at 100-150 m depth as shallow nursery waters start to warm and squid start to mature (Arkhipkin et al., 2004b). In autumn (March-May), the ASC move inshore to spawn with peak spawning occurring in May to June (Hatfield and Desclers, 1998). Squid of the SSC have a markedly different life history. From December-February paralarvae and juveniles stay inshore, gradually moving offshore during autumn and usually finishing their offshore migrations in May-June. The equality in temperatures from shallow sites to depths of 200 m in late autumn (April-May) allows this cohort to penetrate to deeper than the ASC. With winter cooling in shallow sites and the formation of a warm layer at 150-250 m, squid are restricted to this warm water layer and remain on feeding grounds (with no inshore migration) until the end of October, when they rapidly return to shallow depths to spawn (Arkhipkin et al., 2013; Arkhipkin et al., 2004b).

For both cohorts, ontogenetic patterns in mean Sr:Ca concentration over time are consistent with a negative relationship with temperature, when taking into account this lifecycle. For the ASC, the general pattern across the statolith microstructure is an increase in Sr:Ca ratio with a corresponding decrease during late summer (Fig. 4B). The increase in concentration occurs synonymously with the timing of the offshore migration to cooler deeper waters, as would be expected if a negative relationship with temperature existed. At depths where squid are feeding, i.e. at ~150 m, delayed warming occurs in March. Assuming a negative relationship with temperature, reduction in Sr:Ca from February- March corresponds to an increase in near bottom water temperatures on their feeding grounds during this period. Further reductions in the Sr:Ca ratio correspond to a further increase in temperature as the squid undergo inshore migrations to shallower warmer waters in March - May.

The Sr:Ca elemental profile for the SSC is also consistent with a negative relationship with temperature (Fig. 4B). After the initial peak, Sr:Ca concentration progressively increases over time, consistent with the gradual migration of this cohort down the shelf into deeper and cooler waters. As samples were all collected prior to October (when this cohort undergoes its inshore migration), there is no return migration (if there were a negative relationship, a decrease in Sr:Ca ratio as squid move inshore to warmer waters) evident in the elemental profile. It is therefore likely that the elemental incorporation of strontium into statoliths is linked to the physiochemical properties of the ambient environment.

However, a negative correlation between Sr:Ca and temperature is not consistent with the sharp increase in concentration observed in the first five weeks of life when the squid do not undergo extensive migrations and are therefore unlikely to be exposed to such high temperature variability (Fig. 4B). As the majority of biological sampling of *D.gahi* takes place on fishing grounds, early ontogenetic phases prior to the size at which individuals recruit into the fishery (~6 months of age) have not been studied in such detail (Hatfield and Rodhouse, 1994). Factors driving this phenomenon during the first 5 weeks of life are therefore unclear. This pattern may be a result of the interactive effects of several factors, as during this period of ontogeny, squid are undergoing rapid development and significant morphological changes that are likely to affect elemental incorporation. In addition, changes in salinity and temperature are pronounced in the shallow waters where squid hatch (15-30 m) and where their nursery

403 grounds are found (up to 70 m depth) compared to their offshore feeding grounds (> 100 m [Arkhipkin
404 et al., 2013]). A combination of intrinsic and extrinsic factors is likely to be contributing to the observed
405 patterns during this transitional period.

406 *3.3 Ba:Ca ratios*

407 Ontogenetic variation in mean Ba:Ca concentration for both cohorts (ASC and SSC) and consecutive
408 years (2014 and 2015) is shown in Fig. 4D. An increase in Ba:Ca concentration, though not as
409 substantial as for the Sr:Ca ratio, is evident in the first 5 weeks of life for both cohorts and both years.
410 Following this common pattern, Ba:Ca ratio gradually increases for the ASC followed by a
411 corresponding decrease, similar to the pattern observed in the Sr:Ca elemental pattern. Comparison of
412 GAMM smoothers for Ba and Sr indicates that the trends observed in the ASC for both elemental
413 profiles are similar (Fig. 3). Ba:Ca ratio increases for the SSC throughout ontogeny, with a plateau in
414 the elemental signature during March-April.

415 Ontogenetic variation in the concentration of Ba:Ca was substantially different for each cohort (Fig.
416 4C). Thus, as with strontium, it is likely that the Ba:Ca ratios may be useful as a natural tag to
417 distinguish between cohorts. Similar results were reported in Arbuckle and Wormuth (2014), who
418 found Ba:Ca patterns across the statolith microstructure to be highly variable among different sub-
419 groups (based on geographic location).

420 Barium has a nutrient-type distribution in the ocean, with concentration increasing with depth, or
421 indicating upwelling events (Lea et al., 1989). Concentration of Ba in the surrounding seawater has
422 been shown experimentally to be an important factor contributing to the uptake of Ba in fish otoliths
423 (Walther and Thorrold, 2006) and has been inferred to be an important factor for uptake of Ba in
424 cephalopod statoliths (Arkhipkin et al., 2004a), with Ba uptake increasing with depth. As well as water
425 chemistry, temperature has been proposed to be an important factor affecting uptake of barium into
426 biogenic aragonites. Laboratory experiments under different temperature and salinity conditions
427 indicated no relationship with salinity and a negative relationship between temperature and Ba:Ca ratios
428 for statoliths of the cuttlefish *S. officinalis* (Zumholz et al., 2007a; Zumholz, 2006). Although no diet

429 effects have been detected in cephalopods thus far (Zumholz, 2006), interactive effects of food quantity,
430 temperature and life history stage on Ba:Ca uptake have been shown experimentally for the damselfish
431 *A. polyacanthus* (Walther et al., 2010).

432 Given that the ontogenetic patterns for Ba:Ca are similar to those of Sr:Ca for both cohorts, it is likely
433 that Ba:Ca ratios (Fig. 4D) also conform to a negative relationship with temperature (Fig. 4A). The
434 timing of the offshore ontogenetic migration of the ASC into colder deeper waters is concomitant with
435 an increase in Ba:Ca concentration. The timing of the subsequent decrease in elemental concentration
436 corresponds to the timing of the ASC's inshore migration to their warmer shallower spawning habitat.
437 The SSC, as with the Sr:Ca elemental signature, shows a gradual increase in Ba:Ca concentration
438 corresponding to their offshore migration. Unlike the SSC, there is a plateau during March-April
439 synonymous with the period of time when squid have arrived on their shared feeding grounds, followed
440 by further increase in Ba:Ca concentration during late autumn when equality of temperatures allows for
441 penetration into deeper cooler water (Arkhipkin et al., 2004b). The plateau in the elemental signature
442 during the period when squid are found at a constant depth suggests that depth (representative of
443 changes in water chemistry) may also play a role in Ba uptake. Laboratory studies in which ambient
444 water concentration and temperature could be experimentally manipulated, would be required to
445 definitively confirm whether either of these factors have an effect on barium uptake in *D,gahi* statoliths.

446

447 *3.4 Inter-annual variation of element:Ca ratios*

448 The interaction between year of collection and cohort had a significant effect on Sr:Ca ratio in the
449 GAMM model. However, year was removed from the GAMM model for barium as its inclusion of year
450 (or its interaction with cohort assignment) did not improve model fit. Visually, the elemental pattern
451 for each cohort (and both elements) was consistent between years showing the same peaks and troughs.
452 However, elemental concentrations (of both elements) were higher for the SSC in June-August 2015
453 than during the same period in 2014. As an example, SSC Sr:Ca ratios for the last week of July were
454 9.82 $mmol.mol^{-1}$ in 2014 and 10.66 $mmol.mol^{-1}$ in 2015. Comparison of near-bottom water

temperatures from 2014 to 2015 ($T_{2015}$-$T_{2014}$) indicate that temperature values in 2015 are more extreme than the previous year (Fig. 5), with warmer temperatures during the first half of the year and comparably colder temperatures in late 2015. The higher Sr:Ca concentrations found in the SSC in 2015 are likely due to individuals experiencing colder temperatures than 2014.

**Figure 5: Near-bottom temperature differences between 2014 and 2015, defined as $T_{2015} - T_{2014}$.**

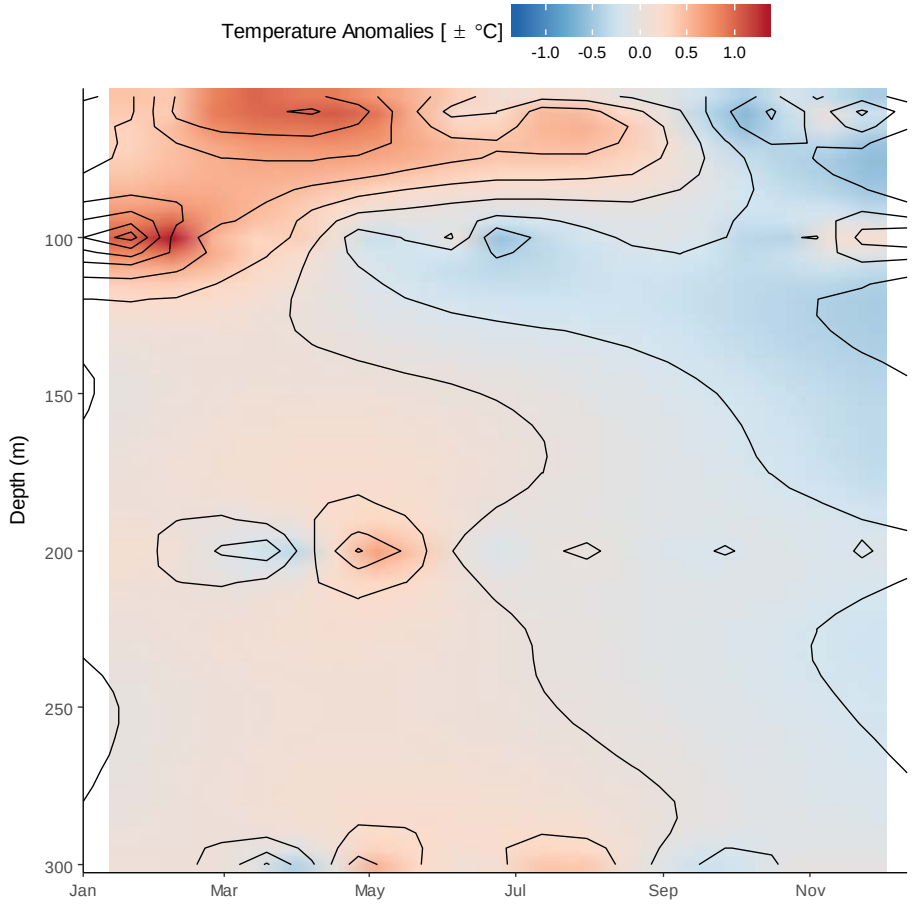


The significant interaction between year and cohort for the strontium model suggest that there are cohort-specific inter-annual differences in the elemental signature. However, this was not the case for barium. Although inter-annual differences in elemental signatures were not significant for barium in the present study, given that only two years have been sampled it would be prudent to sample additional years, to determine whether a pattern exists on a multi-annual basis. If the magnitude of the elemental signal does vary with environmental anomalies, there may be potential predictive applications based on how the chemical signal changes inter-annually with environmental change and how this affects recruitment success in subsequent years. As this species has an annual lifecycle, there is no reservoir of older individuals to buffer the population against poor spawning success. Finer scale predictions of

recruitment would prove invaluable for the real-time stock assessment of this fishery (Winter and Arkhipkin, 2015; Arkhipkin et al., 2008; Beddington et al., 1990).

## 4 Conclusions

The following conclusions can be made from this study:

(1) Each cohort has its own unique elemental fingerprint for both strontium and barium
(2) Analysis of cohort-specific elemental fingerprints in relation to environmental factors indicates a negative relationship between strontium and barium with temperature and also a positive relationship between barium and depth
(3) Life history stage and cohort assignment, have significant effects on Sr:Ca and Ba:Ca concentrations

These results demonstrate that elemental fingerprints of *D. gahi* have applications as a natural tag, discriminating between components of a population. To maximise the potential of this laser ablation method, laboratory based research is required to manipulate environmental factors and assess their effect on elemental incorporation.

## Acknowledgements

This work was supported by the Falkland Islands Government. We thank Dr Simon Chenery, Dr Andy Marriott and the British Geological Survey for assistance with the laser ablation ICP-MS analysis and training and use of their facilities. We are grateful to the scientific observers from the Falkland Islands Fisheries Department for sample collection. We thank the Director of Fisheries, John Barton, and the director of SAERI, Paul Brickle, for supporting this work. We thank Dr Elena Ieno, Dr Andreas Winter and Dr Haseeb Randhawa for their helpful comments that greatly improved the manuscript.

494
495
496
497
498
499
500
501
502
503
504
505
506
507
508
509
510
511

512 **Reference**


513 Agnew, D., Nolan, C., Des Clers, S., 1998. On the problem of identifying and assessing populations of
514 Falkland Island squid Loligo gahi. South African Journal of Marine Science 20 (1), 59-66.

515 Arbuckle, N.S.M., Wormuth, J.H., 2014. Trace elemental patterns in Humboldt squid statoliths from
516 three geographic regions. Hydrobiologia 725 (1), 115-123.

517 Arkhipkin, A.I., 2013. Squid as nutrient vectors linking Southwest Atlantic marine ecosystems. Deep
518 Sea Research Part II: Topical Studies in Oceanography 95, 7-20.

519 Arkhipkin, A.I., Hatfield, E.M.C., Rodhouse, P.G., 2013. *Doryteuthis gahi,* Patagonian Long-Finned
520 Squid. In: Rosa, R., Pierce, G.J. and O'Dor, R.K., (Eds.). Advances in Squid Biology, Ecology
521 and Fisheries. Part I. Nova Biomedical.

522 Arkhipkin, A.I., Middleton, D.A.J., Barton, J., 2008. Management and conservation of a short-lived
523 fishery resource: Loligo gahi around the Falkland Islands. 49 (2), 1243.

524 Arkhipkin, A.I., Campana, S.E., FitzGerald, J., Thorrold, S.R., 2004. Spatial and temporal variation in
525 elemental signatures of statoliths from the Patagonian longfin squid (Loligo gahi). Canadian
526 Journal of Fisheries and Aquatic Sciences 61 (7), 1212-1224.

527 Arkhipkin, A.I., 2005. Statoliths as' black boxes'(life recorders) in squid. Marine and Freshwater
528 Research 56 (5), 573-583.

529 Arkhipkin, A.I., Shcherbich, Z.N., 2012. Thirty years' progress in age determination of squid using
530 statoliths. Journal of the Marine Biological Association of the United Kingdom 92 (06), 1389-
531 1398.

532 Arkhipkin, A.I., Bizikov, V.A., 2000. Role of the statolith in functioning of the acceleration receptor
533 system in squids and sepioids. Journal of zoology 250 (1), 31-55.

534 Arkhipkin, A.I., Grzebielec, R., Sirota, A.M., Remeslo, A.V., Polishchuk, I.A., Middleton, D.A., 2004.
535 The influence of seasonal environmental changes on ontogenetic migrations of the squid
536 Loligo gahi on the Falkland shelf. Fisheries Oceanography 13 (1), 1-9.

537 Arkhipkin, A.I., Rodhouse, P.G., Pierce, G.J., Sauer, W., Sakai, M., Allcock, L., Arguelles, J., Bower,
538 J.R., Castillo, G., Ceriola, L., 2015. World squid fisheries. Reviews in Fisheries Science &
539 Aquaculture 23 (2), 92-252.

540 Beck, J.W., Edwards, R.L., Ito, E., Taylor, F.W., Recy, J., Rougerie, F., Joannot, P., Henin, C., 1992.
541 Sea-surface temperature from coral skeletal strontium/calcium ratios. Science (New York,
542 N.Y.) 257 (5070), 644-647.

543 Beddington, J.R., Rosenberg, A.A., Crombie, J.A., Kirkwood, G.P., 1990. Stock assessment and the
544 provision of management advice for the short fin squid fishery in Falkland Islands waters.
545 Fisheries Research 8 (4), 351-365.

546 Bettencourt, V., Guerra, A., 2000. Growth increments and biomineralization process in cephalopod
547 statoliths. Journal of experimental marine biology and ecology 248 (2), 191-205.

548 Box, G.E., Cox, D.R., 1964. An analysis of transformations. Journal of the Royal Statistical
549 Society.Series B (Methodological) , 211-252.

550 Campana, S.E., 1999. Chemistry and composition of fish otoliths: pathways, mechanisms and
551 applications. Marine ecology.Progress series 188, 263-297.

552 Clarke, M.R., 1978. The cephalopod statolithan-introduction to its form. Journal of the Marine
553 Biological Association of the United Kingdom 58 (3), 701-712.

554 Doubleday, Z.A., Prowse, T.A.A., Arkhipkin, A.I., Pierce, G.J., Semmens, J., Leporati, S.C., Lourenco,
555 S., Quetglas, A., Sauer, W., Gillanders, B.M., 2016. Global Proliferation of Cephalopods.
556 Current Biology Magazine 26 (10), 406-407.

557 Gillanders, B.M., 2005. Using elemental chemistry of fish otoliths to determine connectivity between
558 estuarine and coastal habitats. Estuarine, Coastal and Shelf Science 64 (1), 47-57.

559 Gillikin, D.P., Lorrain, A., Paulet, Y., André, L., Dehairs, F., 2008. Synchronous barium peaks in high-
560 resolution profiles of calcite and aragonite marine bivalve shells. Geo-Marine Letters 28 (5),
561 351-358.

562 Gilly, W., Markaida, U., Baxter, C., Block, B., Boustany, A., Zeidberg, L., Reisenbichler, K., Robison,
563 B., Bazzino, G., Salinas, C., 2006. Vertical and horizontal migrations by the jumbo squid
564 Dosidicus gigas revealed by electronic tagging. Marine Ecology Progress Series 324, 1-17.

565 Hatfield, E.M.C., 1991. Post-recruit growth of the Patagonian squid Loligo gahi (D'Orbigny). Bulletin
566 of Marine Science 49 (1-2), 349-361.

567 Hatfield, E.M.C., Rodhouse, P.G., Porebski, J., 1990. Demography and distribution of the Patagonian
568 squid (Loligo gahi D'Orbigny) during the austral winter. ICES Journal of Marine Science 46
569 (3), 306-312.

570 Hatfield, E., Rodhouse, P., 1994. Distribution and abundance of juvenile Loligo gahi in Falkland Island
571 waters. Marine Biology 121 (2), 267-272.

572 Hatfield, E., Des Clers, S., 1998. Fisheries management and research for Loligo gahi in the Falkland
573 Islands. California Cooperative Oceanic Fisheries Investigations Report 39, 81-91.

574 Hunsicker, M.E., Essington, T.E., Watson, R., Sumaila, U.R., 2010. The contribution of cephalopods
575 to global marine fisheries: can we have our squid and eat them too? Fish and Fisheries 11 (4),
576 421-438.

577 Ikeda, Y., Arai, N., Kidokoro, H., Sakamoto, W., 2003. Strontium: calcium ratios in statoliths of
578 Japanese common squid Todarodes pacificus (Cephalopoda: Ommastrephidae) as indicators
579 of migratory behavior. Marine Ecology Progress Series 251, 169-179.

580 Jackson, G., Forsythe, J., 2002. Statolith age validation and growth of Loligo plei (Cephalopoda:
581 Loliginidae) in the north-west Gulf of Mexico during spring/summer. Journal of the Marine
582 Biological Association of the UK 82 (04), 677-678.

583 Jackson, G., Arkhipkin, A., Bizikov, V., Hanlon, R., 1993. Laboratory and field corroboration of age
584 and growth from statoliths and gladii of the loliginid squid Sepioteuthis lessoniana (Mollusca:
585 Cephalopoda). Recent advances in cephalopod fisheries biology.Tokai University Press,
586 Tokyo , 189-199.

587 Laptikhovsky, V., Arkhipkin, A., Brickle, P., 2010. Squid as a resource shared by fish and humans on
588 the Falkland Islands' shelf. Fisheries Research 106 (2), 151-155.

589 Lea, D.W., Shen, G.T., Boyle, E.A., 1989. Coralline barium records temporal variability in equatorial
590 Pacific upwelling. Nature 340 (6232), 373-376.

591 Limbeck, A., Galler, P., Bonta, M., Bauer, G., Nischkauer, W., Vanhaecke, F., 2015. Recent advances
592 in quantitative LA-ICP-MS analysis: challenges and solutions in the life sciences and
593 environmental chemistry. Analytical and bioanalytical chemistry 407 (22), 6593-6617.

594 Lipinski, M., 1979. Universal maturity scale for the commercially important squids. The results of
595 maturity classification of the Illexo illecebrosus population for the years 1973–1977.
596 Int.Commun.Northw.Atl.Fish 40.

597 Lipinski, M., Durholtz, M., Underhill, L., 1998. Field validation of age readings from the statoliths of
598 chokka squid (Loligo vulgaris reynaudii d'Orbigny, 1845) and an assessment of associated
599 errors. ICES Journal of Marine Science 55 (2), 240-257.

600 Liu, B.L., Chen, X.J., Chen, Y., Tian, S.Q., 2013. Geographic variation in statolith trace elements of
601 the Humboldt squid, Dosidicus gigas, in high seas of Eastern Pacific Ocean. Marine Biology
602 160 (11), 2853-2862.

603 Liu, B.L., Cao, J., Truesdell, S.B., Chen, Y., Chen, X.J., Tian, S.Q., 2016. Reconstructing cephalopod
604 migration with statolith elemental signatures: a case study using Dosidicus gigas. Fisheries
605 Science 82 (3), 425-433.

606 Liu, B., Chen, X., Fang, Z., Hu, S., Song, Q., 2015. A preliminary analysis of trace-elemental signatures
607 in statoliths of different spawning cohorts for Dosidicus gigas off EEZ waters of Chile. Journal
608 of Ocean University of China 14 (6), 1059-1067.

609 Martin, G.B., Thorrold, S.R., 2005. Temperature and salinity effects on magnesium, manganese, and
610 barium incorporation in otoliths of larval and early juvenile spot Leiostomus xanthurus. Marine
611 Ecology Progress Series 293, 223-232.

612 Miller, J., 2011. Effects of water temperature and barium concentration on otolith composition along a
613 salinity gradient: implications for migratory reconstructions. Journal of experimental marine
614 biology and ecology 405 (1), 42-52.

615 Mooney, C., Kingsford, M., 2012. Sources and movements of Chironex fleckeri medusae using
616 statolith elemental chemistry. Hydrobiologia 690 (1), 269-277.

617 Patterson, K.R., 1988. Life history of Patagonian squid Loligo gahi and growth parameter estimates
618 using least-squares fits to linear and von Bertalanffy models. Marine Ecology Progress Series.
619 47 (1), 65-74.

620 Pecl, G.T., Tracey, S.R., Danyushevsky, L., Wotherspoon, S., Moltschaniwskyj, N.A., 2011. Elemental
621 fingerprints of southern calamary (Sepioteuthis australis) reveal local recruitment sources and
622 allow assessment of the importance of closed areas. Canadian Journal of Fisheries and Aquatic
623 Sciences 68 (8), 1351-1360.

624 Piatkowski, U., Pütz, K., Heinemann, H., 2001. Cephalopod prey of king penguins (Aptenodytes
625 patagonicus) breeding at Volunteer Beach, Falkland Islands, during austral winter 1996.
626 Fisheries Research 52 (1), 79-90.

627 Pierce, G.J., Portela, J., 2014. Fisheries production and market demand. In: Anonymous Cephalopod
628 Culture. Springer.

629 Radtke, R.L., Kinzie, R.A., Folsom, S.D., 1988. Age at recruitment of Hawaiian freshwater gobies.
630 Environmental Biology of Fishes 23 (3), 205-213.

631 Radtke, R., 1983. Chemical and structural characteristics of statoliths from the short-finned squid Illex
632 illecebrosus. Marine Biology 76 (1), 47-54.

633 Radtke, R., Shafer, D., 1992. Environmental sensitivity of fish otolith microchemistry. Marine and
634 Freshwater Research 43 (5), 935-951.

635 Smith, S.V., Buddemeier, R.W., Redalje, R.C., Houck, J.E., 1979. Strontium-calcium thermometry in
636 coral skeletons. Science (New York, N.Y.) 204 (4391), 404-407.

637 Team, R.C., 2016. R: A language and environment for statistical computing.Vienna: R Foundation for
638 Statistical Computing; 2014 .

639 Thorrold, S.R., Jones, G.P., Hellberg, M.E., Burton, R.S., Swearer, S.E., Neigel, J.E., Morgan, S.G.,
640 Warner, R.R., 2002. Quantifying larval retention and connectivity in marine populations with
641 artificial and natural markers. Bulletin of Marine Science 70 (1), 291-308.

642 Townsend, D.W., Radtke, R.L., Corwin, S., Libby, D.A., 1992. Strontium: calcium ratios in juvenile
643 Atlantic herring Clupea harengus L. otoliths as a function of water temperature. Journal of
644 experimental marine biology and ecology 160 (1), 131-140.

645 Wang, C., Geffen, A.J., Nash, R.D., 2012. Geographical variations in the chemical compositions of
646 veined squid Loligo forbesi statoliths. Zoological Studies 51 (6), 755-761.

647 Warner, R.R., Hamilton, S.L., Sheehy, M.S., Zeidberg, L.D., Brady, B.C., Caselle, J.E., 2009.
648 Geographic variation in natal and early larval trace-elemental signatures in the statoliths of the
649 market squid Doryteuthis (formerly Loligo) opalescens. Marine Ecology Progress Series 379,
650 109-121.

651 Winter, A., Arkhipkin, A., 2015. Environmental impacts on recruitment migrations of Patagonian
652 longfin squid (Doryteuthis gahi) in the Falkland Islands with reference to stock assessment.
653 Fisheries Research 172, 85-95.

654 Wood, S., 2006. Generalized Additive Models: An Introduction with R. CRC Press.

655 Wood, S.N., 2003. Thin plate regression splines. Journal of the Royal Statistical Society: Series B
656 (Statistical Methodology) 65 (1), 95-114.

657 Zacherl, D.C., Manríquez, P.H., Paradis, G., Day, R.W., Castilla, J.C., Warner, R.R., Lea, D.W.,
658 Gaines, S.D., 2003. Trace elemental fingerprinting of gastropod statoliths to study larval
659 dispersal trajectories. Marine Ecology Progress Series 248, 297-303.

660 Zumholz, K., Klügel, A., Hansteen, T., Piatkowski, U., 2007. Statolith microchemistry traces
661 environmental history of the boreoatlantic armhook squid Gonatus fabricii. Marine Ecology
662 Progress Series 333, 195-204.

663 Zumholz, K., Hansteen, T.H., Piatkowski, U., Croot, P.L., 2007. Influence of temperature and salinity
664 on the trace element incorporation into statoliths of the common cuttlefish (Sepia officinalis).
665 Marine Biology 151 (4), 1321-1330.

666 Zumholz, K., Hansteen, T.H., Klügel, A., Piatkowski, U., 2006. Food effects on statolith composition
667 of the common cuttlefish (Sepia officinalis). Marine Biology 150 (2), 237-244.

668 Zuur, A.F., Ieno, E.N., 2016. A protocol for conducting and presenting results of regression-type
669 analyses. Methods in Ecology and Evolution 7 (6), 636-645.

670 Zuur, A.F., Ieno, E.N., Elphick, C.S., 2010. A protocol for data exploration to avoid common statistical
671 problems. Methods in Ecology and Evolution 1 (1), 3-14.